Journal of Engineering and Sustainable Development
Vol. 22, No.02 (Part-5), March 2018
ISSN 2520-0917
10.31272/jeasd.2018.2.68

ECO- FRIENDLY POLYSULFONE TRICOMPOSITE FOR DUAL PROTECTION FROM UV RAYS

* Dr. Raouf Mahmood Raouf[1], Khalid Murshed Owaid[2], Nisreen Mizher Rahma[3]

1) Lecturer, Material Engineering Department, Mustansiriyah University, Baghdad, Iraq.
2) Assist Prof., Material Engineering Department, Mustansiriyah University, Baghdad, Iraq.
3) Assist Lecturer, Material Engineering Department, Mustansiriyah University, Baghdad, Iraq

Abstract: A Transparent nanocomposite consist of polysulfone (PSF), cellulose acetate butyrate (CAB) and nano indium oxide (nanoIn_2O_3) was prepared by melting and re-molding so as to safeguard from the impact of ultraviolet rays. By means of scanning electron microscope (SEM), X-ray diffraction (XRD), UV-Vis spectroscopy, dynamic mechanical analysis (DMA) and thermogravimetric analysis (TGA), the morphological, optical, mechanical and thermal properties were studied. As we reported before that PSF/0.2%CAB implies low ultraviolet light absorption for PSF and CAB transparent blend. In the present study, we investigated the effect of nanoIn_2O_3 on the characteristics of PSF/0.2%CAB/nanoIn_2O_3 Tricomposite. The results showed that the inorganic nano particles are well dispersed in the PSF matrix without macro phase separation, as well as assisting to spread the organic component CAB. The UV-Vis spectroscopy showed that 0.02%nanoIn_2O_3 is able to shield PSF from UV radiation. So, we've got dual protection transparent eco-friendly nanocomposite from UV rays and is also able to protect the surfaces from the impact of these rays if used as a protection them. The XRD pattern of pure PSF clarified that there is a noticeable decrease in the bundle peaks in bi-composite and Tricomposite pattern. Furthermore, the Tricomposite showed high stability to temperatures lower than T_g.

Keywords: *Indium Oxide nanoparticles (nanoIn_2O_3), Cellulose acetate butyrate (CAB), Polysulfone (PSF), Ultraviolet.*

ثلاثي المركب من البوليسلفون صديق للبيئة لغرض الحماية المزدوجة من الاشعة فوق البنفسجية

الخلاصة:تم تحضير مركب نانوكومبوسيت شفاف يتكون من بوليسولفون (PSF)، سليلوز اسيتيت بيوتريت (CAB) وأكسيد النانو إنديوم (nanoIn_2O_3) عن طريق الصهر وإعادة صب وذلك من أجل الحماية من تأثير الأشعة فوق البنفسجية. لقد تم دراسة الخصائص البنائية والبصرية والميكانيكية والحرارية من خلال مسح المجهر الإلكتروني (SEM)، حيود الأشعة السينية (XRD)، التحليل الطيفي للأشعة فوق البنفسجية(UV-VIS)، التحليل الميكانيكي الديناميكي (DMA) والتحليل الحراري الحراري (TGA). لقد ذكرنا من قبل أن PSF/0.2%CAB يظهر امتصاص ضعيف للاشعة فوق البنفسجية للمزيج الشفاف المتكون من (PSF) و (CAB) .في هذه الدراسة، قمنا بتحقيق تأثير nanoIn_2O_3 على خصائص PSF/0.2%CAB/nanoIn_2O_3 ثلاثي المركب. وأظهرت النتائج أن جزيئات النانو غير العضوية المنتشرة بشكل جيد في مصفوفة البوليسلفون(PSF) ساعدت في تقليل فصل الطور جاهري، فضلا عن مساعدتها في نشر المكون العضوي (CAB). أظهر التحليل الطيفي للأشعة فوق البنفسجية (UV-VIs) أن نسبة 0.02٪ من nanoIn_2O_3 قادرة على حماية (PSF) من الأشعة فوق البنفسجية. لذلك، اصبح لدينا حماية مزدوجة شفافة صديقة للبيئة (نانوكومبوسيت) من الأشعة فوق البنفسجية، بالاضافة الى القدرة على حماية الأسطح من تأثير هذه الأشعة إذا ما استخدمت كحماية لهم. أوضح نموذج (XRD) ل (PSF) النقي أن هناك انخفاضًا ملحوظًا في القمم المجمعة في نمط ثنائي المركب و ثلاثي المركب .علاوة على ذلك ، أظهر ثلاثي المركب ثبات عالي لدرجات حرارة أقل من T_g.

*Corresponding Author raoufmahmood@uomustansiriyah.edu.iq

1. Introduction

Numerous studies have included nanocomposite materials based on a polymer matrix and inorganic materials in order to overcome the drawbacks or to extract the polymers with new functionality. Polymer/oxide nanoparticles are one of the most important nanocomposites that have been applied for augmenting demands of optical filtration, ophthalmic lenses and other optical applications. Often oxide nanoparticles are the basic substance in shielding transparent polymers against UV radiations [1, 2]. An indium oxide nanoparticles (nanoIn_2O_3) are one of inorganic oxide nanoparticles with very interesting optical properties, so it becomes one of our work nanocomposite elements [3, 4]. The nanoIn_2O_3 show a strong absorption below (450 nm) with a well-defined absorbance peak around (280 nm) [5]. It has been used in many applications related to UV rays like near-UV photo detector [3].

Polysulfone (PSF) is a transparent amorphous thermoplastic low yellowness polymer. It was found to be a substitute of polycarbonates. Recently, PSF has been widely used as an important material for optical devices. It characterize by desired optical properties because of sulfone groups and aromatic nuclei. [6, 7]. Chemically, PSF has low moisture absorption and high T_g about (185°C) [8, 9]. Physically, PSF is a rigid, high strength, stiffness and high compaction resistance polymer [10].

Recently, we reported that 0.2%CAB in PSF matrix could make PSF/CAB blend more transparent to ultraviolet and visible rays. Moreover, the presence of CAB in PSF/CAB led to improve the thermal and mechanical properties of the blend [11]. In the present work, we look at the impact of inorganic In_2O_3 nanoparticles on the optical properties of organic PSF for the purpose of obtaining the utmost UV shields for PSF/In_2O_3 nanocomposite. Then study the optical properties of PSF/CAB/nanoIn_2O_3 tricomposite as an integrated whole in order to achieve the goal of the work which is obtaining a dual-performance nanocomposite able to protect itself from the influence of ultraviolet rays in addition to being a protection against these rays. Moreover the thermal, morphological and thermomechanical properties of the samples in addition to optical properties were studied.

2. Experimental

2.1. Materials

Polysulfone (transparent pellets) (M_w ~35,000), cellulose acetate butyrate (white powder) (M_n 12,000) were delivered by Sigma-Aldrich (USA). Indium Oxide nanoparticles (<50nm) (M_w = 277.63) by Aladdin.

2.2. Method

The samples were prepared using twin screw Thermo-Haake Poly Drive Internal Mixer (Germany) (D =19.05 mm) and Hsin-Chi Machinery Co. Ltd. hot press (Taiwan). The materials were dried in a vacuum oven at (50°C) for (4 h) before mixing. Two types of nanocomposites were prepared; the first was binary composites (bi-composite) and

the second was triplex composites (Tricomposites). All nanocomposite samples were prepared in two stages; on the first stage was melt-kneading the polymer pellets in the extruder at a rotation rate of (50 rpm) at (225°C) for (10 min). Then, variable percentage weights of nano/In_2O_3 (0.01%, 0.02%, 0.03%, 0.04% and 0.05%) were added to the molten of PSF. Mixing continued until reaching to constant torque, which took about (10-15 min), this regards to bi-composite samples. In tricomposite 0.2%CAB was added to the molten with same previous steps. The second stage was proceeding the samples in a hot press at (110 KPa) and (225°C) to form a sheet (70 mm × 90 mm, 1 mm/3mm) thick. All samples were transparent and homogeneous in their outward appearance.

2.3. Measurements

The transmittance and absorbance property of the samples was determined at room temperature using ultraviolet-visible (UV-VIS) spectroscopy (Shimadzu UV-3600 spectrophotometer, Japan). The surface topography was obtained out by scanning electron microscopy (SEM) studies on a Hitachi S-3400N (Japan) microscope. The X-ray diffraction (XRD) patterns were collected at room temperature in (20–80°) 2Ɵ range at a scanning speed of (5°/min) using an X-ray diffractometer (Philips/X'Pert Pro Panalytical - PW 3040/60 MPD, Netherlands). Dynamic mechanical analysis (DMA) was made on a PerkinElmer Pyris Diamond (USA) apparatus in tension mode at a frequency of (1 Hz) and a heating rate of (5°C/min) in a liquid nitrogen atmosphere. Thermal gravimetric analysis (TGA) was taken on a TGA/DSC1 STAR System (USA) at a heating rate of (20°C/min) from room temperature to (1000°C) in a continuous highly pure nitrogen atmosphere.

3. Results and Discussion

3.1. UV-VIS Spectroscopy

The absorbance and transmittance curves, in addition to the spectra and the visual appearance of the PSF and PSF/nanoIn_2O_3 nanocomposites are shown in Fig. 1.

The nanoIn_2O_3 concentration in PSF was (0.01, 0.02, 0.03, 0.04 and 0.05%). Fig. 1a shows the relationship between absorbance and concentration for PSF at (268 nm). While the relation between transmittance and concentration at (712.5 nm) is illustrate in Fig. 1b. We mentioned before that pure PSF has absorbance peak in the ultraviolet zone at (268 nm) and transmittance peak at (712.5nm) [11]. It is clear that (0.02%In_2O_3) nanopowder is able to increase the PSF/nanoIn_2O_3 shielding against UV-radiation with rise in transmittance value from (82% to 84.7%). The reduction in the value of absorbance and transmittance with concentration increasing led to discard the concentrations that are higher than 0.02%nanoIn_2O_3 being not serve search requirements, which is getting highest absorbance (shielding) at (268 nm) and transmittance at (712.5nm). The defensive against ultraviolet radiation in PSF/nanoIn_2O_3 composite leads to reduce the breakdown of bonds in the polymeric chain and disintegration over time. So, this will increase the life time of utilization [12]. On the other hand, the increase in optical transmittance in the visible region, especially

at a wavelength of (712.5 nm), will give the bi-composite broader prospects for optical applications. Therefore, 0.02% nanoIn_2O_3 is the best concentration of PSF bi-composite in terms of high absorption in the mid-ultraviolet region and high transmittance within visible region.

The samples started to loss the transparency with nanoIn_2O_3 concentration increasing in PSF. Therefore, the samples with concentrations more than 0.05% were discarded because they did not meet the required purpose.

NanoIn_2O_3 exhibit strong ultraviolet absorption band because of surface plasmon resonance (SPR), which is the coherent excitation of all free electrons within the conduction band. So, (SPR) resulting an in-phase oscillation because the size of nanoIn_2O_3 is smaller than the wave-length of incident radiation [13].

The Tricomposite sample absorbance and transmittance spectrum curve in addition to pure PSF, PSF/0.2%CAB and 0.02%nanoIn_2O_3 were illustrated in Fig. 2.a. The PSF/0.2%CAB/0.02%In_2O_3 Tricomposite has absorbance value locate between PSF/0.2%CAB and PSF/0.02%In_2O_3 on one hand and pure PSF on the other hand. Fig. 2.b shows the absorbance values for the above mentioned samples at (268 nm). The transmittance value of PSF/0.2%CAB/0.02%In_2O_3 Tricomposite at (712.5 nm) decreased to (82.9%) as in Fig. 2.c.

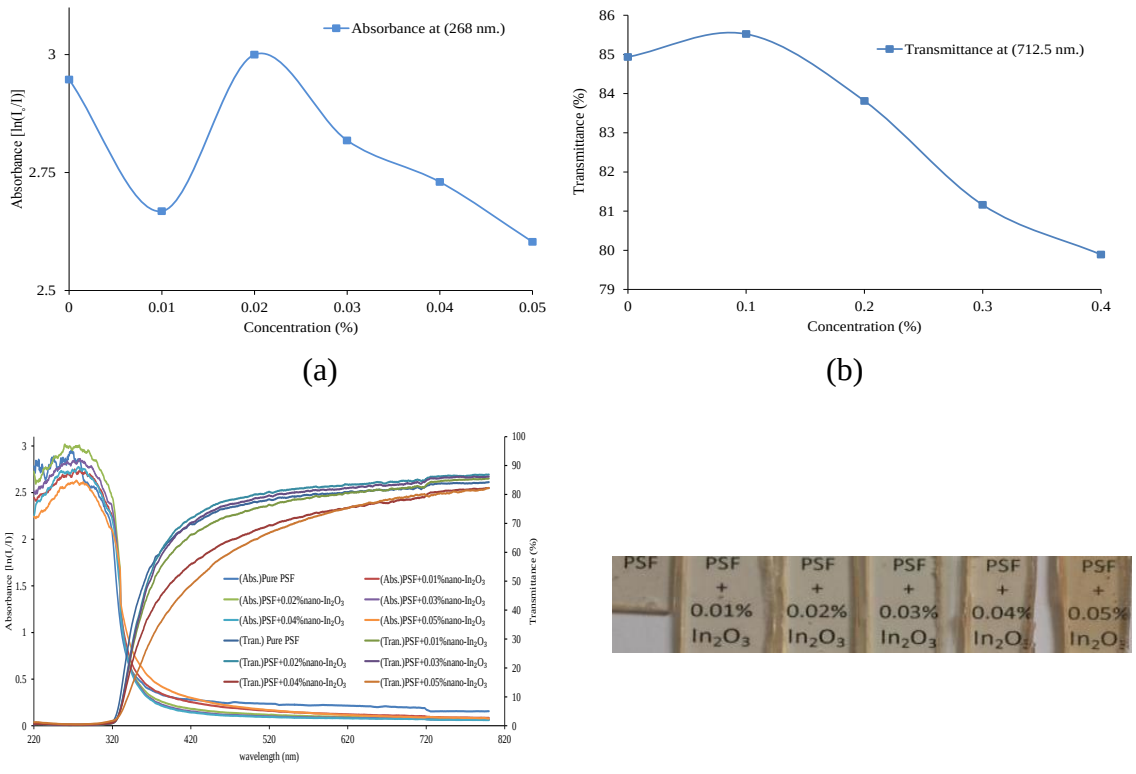

Figure 1. (a) Absorbance of PSF and nanoIn_2O_3 in different concentrations at 268 nm. (b) Transmittance of PSF and nanoIn_2O_3 in different concentrations at 712.5 nm. (c) PSF/ nanoIn_2O_3 absorbance and transmittance spectrum with concentration. (d) PSF/ nanoIn_2O_3 sheets in different transparent concentrations.

In tricomposites curve, (PSF/0.2%CAB/0.02%nanoIn_2O_3), show high ability to shield the UV rays affect, this due to good dispersion of nanoIn_2O_3 in polymer matrix and the ability of nanoparticles to block UV rays. In addition to CAB effect which reduce the intensity of the interaction between the UV rays and the material [14]. So the tricomposite has dual protection to UV rays. It can also use as a UV filter because of the UV blocking feature.

The reduction in transmittance value for Tricomposite sample could be attributed to the polarizability anisotropy in ester groups [15].

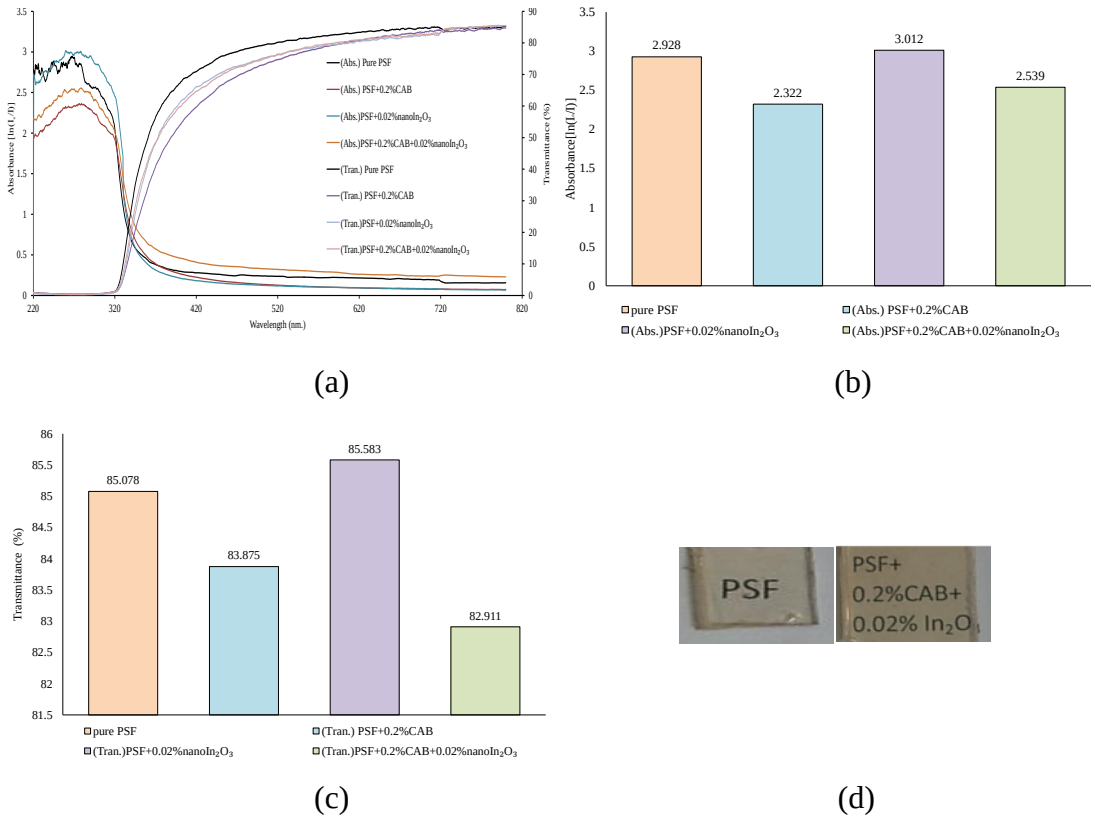

Figure 2: (a) PSF/CAB/ nanoIn_2O_3 absorbance and transmittance spectrum with concentration. (b) The absorbance values for pure PSF, blend and nanocomposites at 268 nm. (c) The transmittance values for pure PSF, blend and nanocomposites at 712.5 nm (d) Pure PSF and PSF/CAB/ nanoIn_2O_3sheets.

3.2. X-Ray Diffraction

X-ray diffraction patterns of pure PSF, blend and nanocomposite in addition to CAB powder and nanoIn_2O_3 powder are reported in Fig. 3. The base PSF is known to be an amorphous polymer with rigid polymer structure. A study on PSF structure with same amorphous material CAB revealed match and absence of lattice peaks in blend, di-composites and tricomposites [16]. But there are different intensities appeared in diffractogrames. The tricomposite PSF+0.2%CAB+0.02%nanoIn_2O_3 has highest intensity which is more than four times of identical pure PSF and PSF/0.2%CAB intensity. Wide scattering peaks (humps) in XRD thermograme are a sign of amorphous material. Where the increase in humps intensities indication of intricate arranges

happened by changes in atomic planes within amorphous structure. So, the structure of PSF+0.2%CAB+0.02%nanoIn_2O_3 composite is more complicated compound [17].

The bundle lattice peaks of crystalline nanoIn_2O_3 powder illustrate the locations and intensities of the peaks with corresponding angles (2Θ°). The significant miller indices identify a cubic structure of nanoIn_2O_3. The wrapping process in the PSF induced nanopowder dispersal, as revealed by the noticeable decrease or disappearance of the bundle peaks in bi-composite and Tricomposite. Notice that the main feature bands of the pure PSF are low intense, so they practically do not interfere with the bundle lattice peaks as seen in Fig. 3 [18].

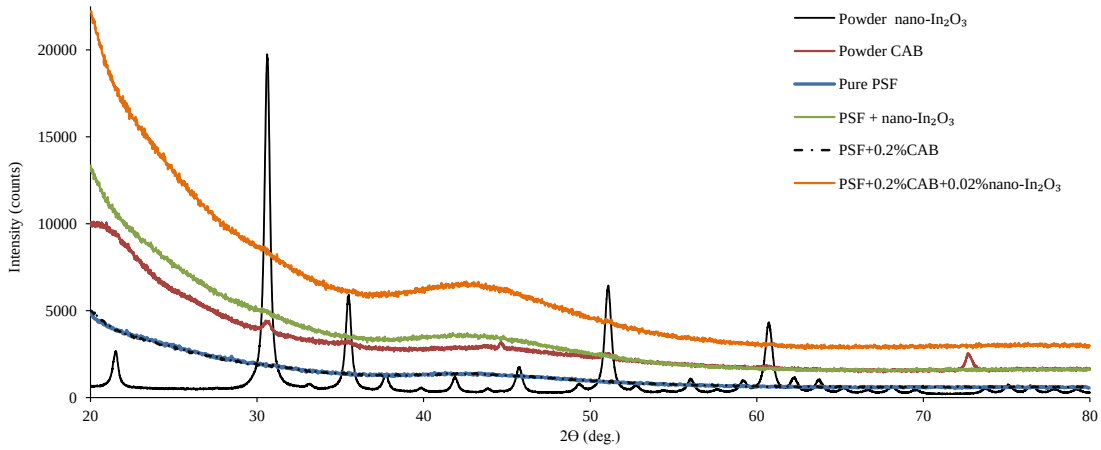

Figure 3. X-Ray diffractogrames of powder nano-In_2O_3, powder CAB, pure PSF, PSF/nanoIn_2O_3, PSF/0.2%CAB and PSF/0.2%CAB/0.02%nanoIn_2O_3

3.3. Scanning Electron Microscopy

The characteristic features of pure PSF, PSF/nanoIn_2O_3 and the PSF/0.2%CAP/0.02%nanoIn_2O_3 nanocomposite obtained from SEM are shown in Fig. 4. The SEM images for each sample are shown at three different magnifications (2, 5, and 10μm). The pure PSF surface images illustrate, unambiguously, uniform morphological features, representing a single material (homopolymer) (Fig. 5.a–c). For bi-composite, the PSF/0.02%nanoIn_2O_3 sample presented morphologies similar to that for pure PSF. So, the interface between PSF and nanoIn_2O_3 is enough for providing miscibility (Fig. 5.d–f). We reported the size reduction of CAB compound in PSF matrix as a result of surface tension which seemed as spherical shapes [11]. The addition of nanoIn_2O_3 assisted CAB particles to liberate from the effect of surface tension and began to spread in the PSF matrix (Fig. 5.g-i). The difference in the interaction between Tricomposite functional components led to an increase or decreases the strength of spread [19, 20].

It can be seen that the inorganic nanoparticles are homogeneous and continuous in the nanocomposite, which is indicative of the formation of interpenetrating PSF and CAB/nanoIn_2O_3 network structure. From the above observations, it can be concluded that in our nanocomposite system there is a good compatibility between the organic and

inorganic components and the inorganic nanoparticles are well dispersed in the PSF matrix in addition to assist in the spread of CAB.

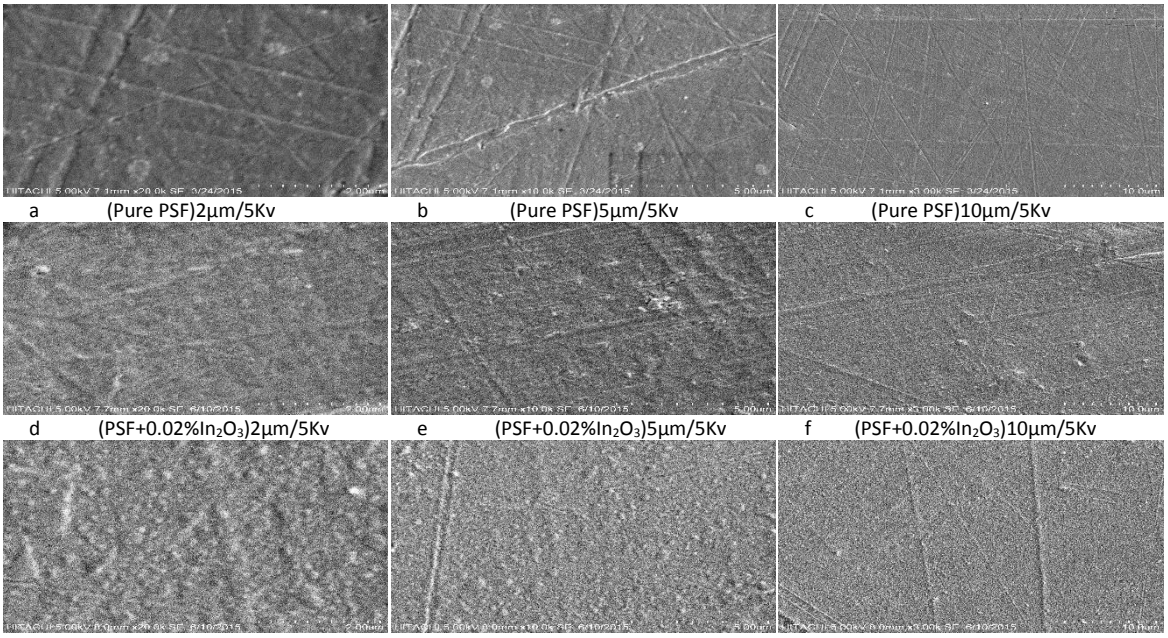

a (Pure PSF)2µm/5Kv b (Pure PSF)5µm/5Kv c (Pure PSF)10µm/5Kv

d (PSF+0.02%In_2O_3)2µm/5Kv e (PSF+0.02%In_2O_3)5µm/5Kv f (PSF+0.02%In_2O_3)10µm/5Kv

g (PSF+0.2%CAB+0.02%nano-In_2O_3)2µm/5Kv h (PSF+0.2%CAB+0.02%nano-In_2O_3)5µm/5Kv i (PSF+0.2%CAB+0.02%nano-In_2O_3)10µm/5Kv

Figure 4. SEM images for pure PSF, PSF/0.02%nanoIn_2O_3 and PSF/0.2%CAB/0.02%nanoIn_2O_3 nanocomposites with different scales bar(a)PSF-2µm.(b)PSF-5µm.(c)PSF-10µm.(d)PSF/0.02%nanoIn_2O_3-2µm.(e) PSF/0.02%nanoIn_2O_3-5µm.(f)PSF/0.02%nanoIn_2O_3-10µm.(g)PSF/0.2%CAB/0.02%nanoIn_2O_3-2µm.(h) PSF/0.2%CAB/0.02%nanoIn_2O_3-5µm.(i) PSF/0.2%CAB/0.02%nanoIn_2O_3-10µm.

3.4. Dynamic Mechanical Analysis

The dynamic mechanical analysis (DMA) is a technique provides information about the mechanical properties of the material below periodic stress by applying a changeable sinusoidal stress under thermal conditions. The technique measures three specific factors; storage modulus E'(energy dissipated), loss modulus E'' (energy stored) and tanδ (phase angle) which is proportional to the ratio of energy dissipated to energy stored per cycle of the applied load [21].

The E' curve in Fig.5.a of pure PSF shows lowest value and the higher is for PSF/0.02%nanoIn_2O_3. On the contrary E'' curve showing high value for pure PSF curve as in Fig.5.b. That means nanoparticles are able to increase the E' value for PSF in composites. In glassy zone, the E' curves for pure PSF and PSF/0.02%nanoIn_2O_3 showed beta relaxation at (45°C), with difference in E' value that PSF/0.02%nanoIn_2O_3 curve is higher than pure PSF Moreover, in glassy zone, the Tricomposite sample showed high stability against applied mechanical load (stress) therefore, the corresponding strain (relaxations) not appeared. It means the fragments of Tricomposites are so immovable that they are incapable to resonate with the oscillatory loads therefore remain stiff. In Tricomposites, the well dispersed nanoIn_2O_3 in addition to interfacial interactions between PSF matrix and nanoIn_2O_3 reduced the molecular motion [22]. The decrease that happened in the value of E'' for bi-composite sample

after adding nanoIn_2O_3 is a testament to the contribution of nanoparticles to improve the sample stiffness. The 0.2%CAB in Tricomposite sample reduced the activation of carbonyl and hydroxyl units considerably in order to give lowest E" value [23].

The peak in tanδ curves for pure PSF and nanocomposites in Fig.5.c represents T_g values. PSF showed an approximate constancy in the T_g values. The sulfone with two adjacent benzene rings in PSF matrix contains a highly conjugated diphenyl structure, with important rigidity of the molecular chains for pure PSF, which led to a high T_g at about (176˚C) [24].

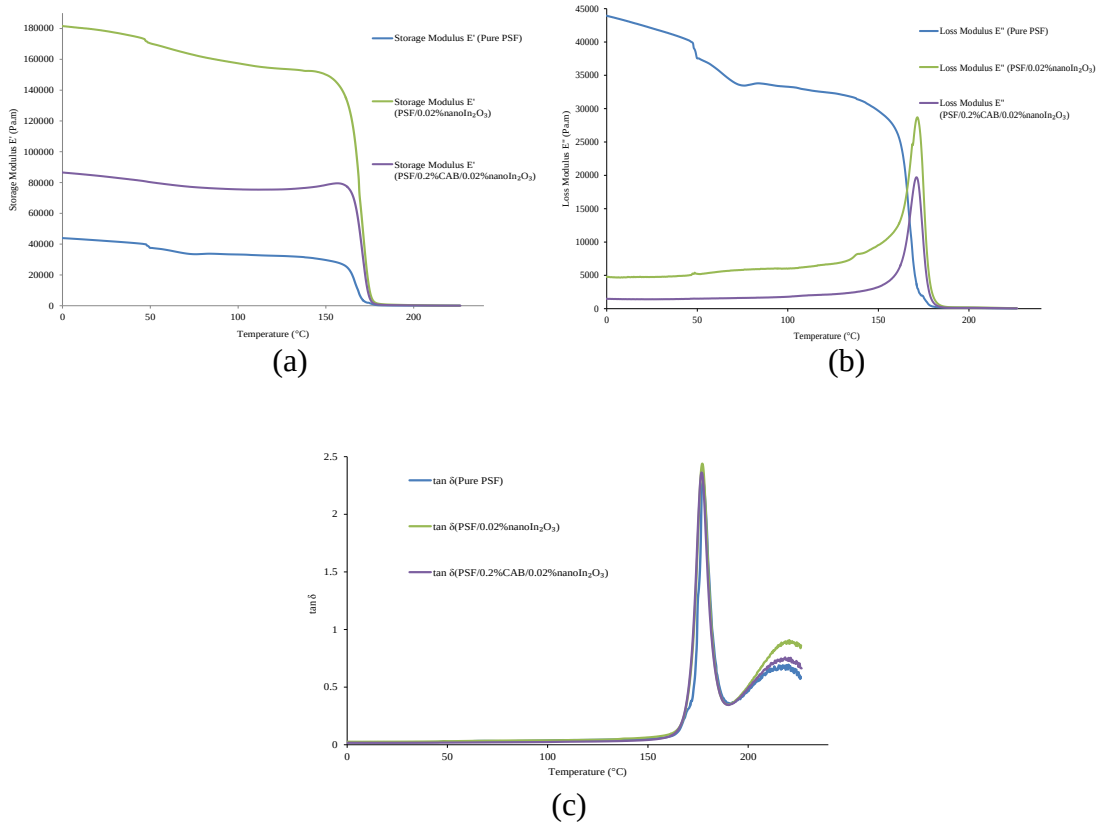

Figure 5: (a) Storage modulus E', (b) loss modulus E" and (c) tan δ trace for pure PSF and PSF/0.02%nanoIn_2O_3 and PSF/0.2%CAB/0.02%nanoIn_2O_3 as a function of temperature by DMA.

3.5. Thermogravimetric Analysis

The thermogravimetric analysis (TGA) and derivative thermogravimetry (DTG) charts for pure PSF, PSF/0.02%nanoIn_2O_3 and the PSF/0.2% CAB/0.02%nanoIn_2O_3 are shown in Fig. 6.a, b, c. All the DTG peaks represent degradation point for each stage.

The TGA diagram of pure PSF shows two thermal degradation stages as an indication of the measurement was carried out under oxidative atmospheres Fig.6,a. The first stage extends from (243.2°C) to (453.2°C) with mid-point temperature (389°C) because of the loss in sulfonic acid groups and the second stage ranges from (455.9°C) to (651.2°C) and mid-point temperature (527.8°C) as a result of carbonization of the degraded residuals (polymeric backbone degradation) [11, 25-27]. The DTG diagram peaks correspond with mid-point temperatures for each stage. The weight loss of pure

PSF first stage amounted to (27.5%) and the second amounted to (52.5%). The TGA diagram of pure PSF shows early thermal degradation start from (89°C to 245°C) due to the residual water bound to the hydrophilic imidazole moieties.

The TGA diagram of PSF/0.02%nanoIn_2O_3 bi-composite divided into two main stages, the first stage from (54°C to 292°C) with mid-point at (94.3°C) attributed to release of the absorbed water and the second from (421.8°C to 680°C) with mid-point at (526.7°C) is corresponding to the degradation of polymer main chains, Fig.6, b [26, 27]. It was reported that the major weight loss stage for nanoIn_2O_3 less than (350°C) is associated with the elimination of physisorption water (physical water adsorption) [28, 29]. While above (400°C) PSF's exhibit almost the same degradation styles though decomposition. Therefore, adding 0.02%nanoIn_2O_3 to pure PSF unable to change the significant peak of TGA around (527°C).

The PSF/0.2%CAB/0.02%nanoIn_2O_3 Tricomposite diagram of TGA and DTG in Fig. 6, c show two significant thermal degradation states, the first starts at (53.2°C) up to (280.2°C) with mid-point temperature at (82.5°C) characterizes bound water evaporation and the second extends from (426.9°C) to (709°C) with mid-point temperature at (528.2°C) signifies the composite backbone degradation. The convergence clearly between PSF/0.2%CAB/0.02%nanoIn_2O_3 and PSF/0.02%In_2O_3 diagram in shape and values could attribute to the disability of CAB to effect on the thermal properties of the composite. The increase in amorphous regions after adding CAB and weakening the impact of the crystalline regions of nanoIn_2O_3 is the reason of thermal degradation peaks creep toward low temperatures [30].

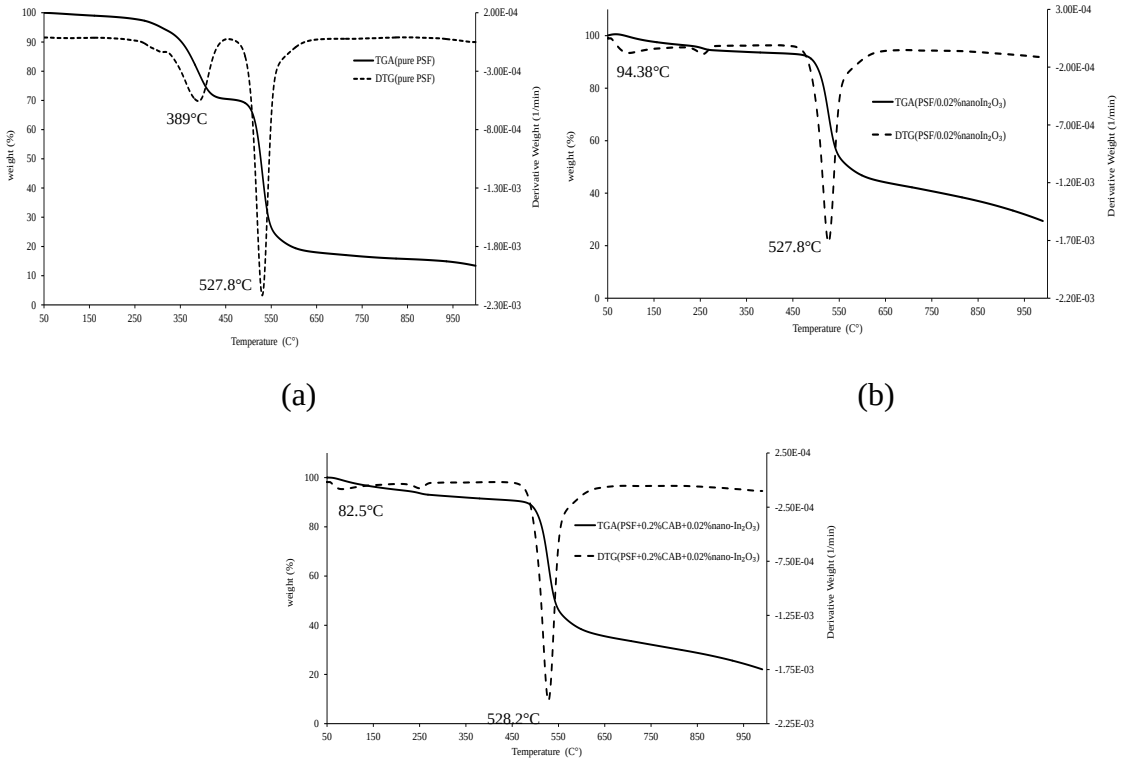

(a) (b)

(c)

Figure 6: TGA- trace for (a) pure PSF (b) PSF/0.02%nanoIn_2O_3 (c) PSF/0.2%CAB/0.02%nanoIn_2O_3.

4. Conclusions

In this work, it was reached to an eco-friendly PSF/CAB/nanoIn_2O_3 Tricomposite able to protect itself from the impact of ultraviolet rays in addition to using it as a shield against these rays. The nanocomposite consists of 0.2%CAB and 0.02% nanoIn_2O_3 in PSF matrix. The results showed that the presence of nanoIn_2O_3 increase the value of storage modulus to more than four times the value of pure PSF. It was noted that there is a thermal stability originated from good diffusion of In_2O_3 nanoparticles in a composite structure. The amorphous structure of PSF maintains even after the addition of nanoIn_2O_3.

5. References

1. Hu Y, Zhou S, & Wu L (2009). "*Surface mechanical properties of transparent poly (methyl methacrylate)/zirconia nanocomposites prepared by in situ bulk polymerization".* Polymer, 50(15):3609-3616.
2. Singhal A, *et al.* (2013). "*UV-shielding transparent PMMA/In_2O_3 nanocomposite films based on In_2O_3"nanoparticles*. RSC Advances 3(43):20913-20921.
3. Shao D, Qin L, & Sawyer S (2012). *" responsivity, bandpass near-UV photodetector fabricated from PVA-nanoparticles on a GaN substrate".* Photonics Journal, *IEEE* 4(3):715-720.
4. Zhang D, *et al.* (2004). "*Detection of NO2 down to ppb levels using individual and multiple In_2O_3 nanowire devices".* Nano letters, 4(10):1919-1924.
5. Maensiri S, *et al.* (2008)."*Indium oxide (In_2O_3) nanoparticles using Aloe vera plant extract: Synthesis and optical properties".* J Optoelectron Adv Mater, 10:161-165.
6. Marin L & Perju E (2009). "*Polysulfone as polymer matrix for a novel polymer-dispersed liquid crystals system".* Phase Transitions, 82(7):507-518.
7. Perju E, Marin L, Grigoras VC, & Bruma M (2011). "*Thermotropic and optical behaviour of new PDLC systems based on a polysulfone matrix and a cyanoazomethine liquid crystal".* Liquid Crystals, 38(7):893-905.
8. El-Hibri MJ & Weinberg SA (2001). "*Polysulfones".* Encyclopedia of Polymer Science and Technology. John Wiley & Sons.
9. Malek CK & Duffait R (2007). "*Packaging using hot-embossing with a polymeric intermediate mould".* The International Journal of Advanced Manufacturing Technology, 33(1-2):187-190.
10. Bourdelais RP & Greener J (2006). "*Microstructured film containing polysulfone polymer".* (Patents).
11. Raouf R, Wahab Z, Ibrahim N, & Talib Z (2015). "*Polysulfone/Cellulose Acetate Butyrate Environmentally Friendly Blend to minimize the Impact of UV Radiation".* J Material Sci Eng, 5(219):2169-0022.100021.
12. Gesner B & Kelleher P (1968). "*Thermal and photo-oxidation of polysulfone".* Journal of Applied Polymer Science, 12(5):1199-1208.
13. Pokropivny V (2007). "*Introduction to nanomaterials and nanotechnology*", Tartu University Press. Ukraine.
14. Raouf RM, Wahab ZA, Ibrahim NA, Talib ZA, & Chieng BW (2016). "*Miscible Transparent Polymethylmethacrylate/Cellulose Acetate Propionate Blend: Optical, Morphological, and Thermomechanical Properties".* BioResources, 11(2):3466-3480.

15. Yamaguchi M, *et al.* (2009). "*Extraordinary wavelength dispersion of orientation birefringence for cellulose esters".* Macromolecules, 42(22):9034-9040.
16. Margolis J (2012). "Conductive polymers and plastics*".* Springer Science & Business Media. New York.
17. Arribas P., Khayet M., Garcia-Payo M. C., & Gil L. (2014). "*Self-sustained electro-spun polysulfone nano-fibrous membranes and their surface modification by interfacial polymerization for micro-and ultra-filtration".* Separation and Purification Technology, 138, 118-129..
18. Diez-Pascual AM, *et al.* (2010). "*High performance PEEK/carbon nanotube composites compatibilized with polysulfones-I. Structure and thermal properties"*. Carbon. 48(12):3485-3499.
19. Guo H, *et al.* (1998). "*Compatibilizing effects of block copolymers in low-density polyethylene/polystyrene blends"*. Polymer, 39(12):2495-2505.
20. Robeson L (2014). "*Historical Perspective of Advances in the Science and Technology of Polymer Blends"*. Polymers, 6(5):1251-1265.
21. Menard KP (2008). "*Dynamic mechanical analysis: a practical introduction"* ,CRC press. USA.
22. Liu C, *et al.* (2011). "*Enhancement of mechanical properties of poly (vinyl chloride) with polymethyl methacrylate-grafted halloysite nanotube"*. Express Polym Lett., 5(7):591-603.
23. Merenga AS & Katana G (2010). "*Dynamic mechanical analysis of PMMA-cellulose blends"*. International Journal of Polymeric Materials, 60(2):115-123.
24. Zhang J & He J (2002). "*Interfacial compatibilization for PSF/TLCP blends by a modified polysulfone"*. Polymer, 43(4):1437-1446.
25. Momeni S & Pakizeh M (2013). "*Preparation, characterization and gas permeation study of PSf/MgO nanocomposite membrane"*. Brazilian Journal of Chemical Engineering, 30(3):589-597.
26. Krishnaswamy RK, Wadud SEB, & Baird DG (1999). "*Influence of a reactive terpolymer on the properties of in situ composites based on polyamides and thermotropic liquid crystalline polyesters"*. Polymer, 40(3):701-716.
27. Liu L, *et al.* (2015). "*Novel quaternized mesoporous silica nanoparticle modified polysulfone-based composite anion exchange membranes for alkaline fuel cells"*. RSC Advances, 5(54):43381-43390.
28. Souza E, Rey J, & Muccillo E (2009). "*Synthesis and characterization of spherical and narrow size distribution indium oxide nanoparticles"*. Applied Surface Science, 255(6):3779-3783.
29. Maensiri S, *et al.* (2008). "*Indium oxide (In2O3) nanoparticles using Aloe vera plant extract: Synthesis and optical properties"*. J Optoelectron Adv Mater, 10:161-165.
30. El-Zaher NA, Melegy MS, & Guirguis OW (2014). "*Thermal and Structural Analyses of PMMA/TiO_2 Nanoparticles Composites"*. Natural Science, 2014(6):859-870.